

Absorption of  $\mu^-$  Mesons in  $C^{12}\dagger$ H. V. ARGO, F. B. HARRISON, H. W. KRUSE, AND A. D. MCGUIRE  
*Los Alamos Scientific Laboratory, University of California, Los Alamos, New Mexico*

(Received November 25, 1958)

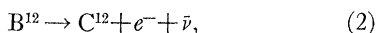
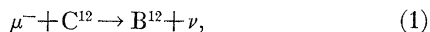
It is known that there is a strong similarity between the electron-nucleon and electron-muon weak interactions. This paper is a report on an experimental investigation of the third leg of the triangle, the muon-nucleon interaction. The absorption of negative cosmic-ray muons stopped in  $C^{12}$  was studied, and the probability per second of absorption resulting in the formation of  $B^{12}$  in the ground state was measured and found to be  $9050 \pm 950 \text{ sec}^{-1}$ . This is compared to the known rate of  $\beta$  decay of  $B^{12}$  to the ground state of  $C^{12}$ ,  $33.2 \pm 0.65 \text{ sec}^{-1}$ . The ratio of the rates is  $273 \pm 29$ . In the allowed approximation, the nuclear matrix elements for the two processes are the same, and the ratio of the rates can be calculated in terms of the ratio of the coupling constants without assuming a nuclear model. The short wavelength of the neutrino emitted in  $\mu$  absorption (13 fermis) causes forbidden matrix elements to make an important contribution to the  $\mu$ -absorption rate, so that the theoretical prediction is dependent on the nuclear model. Within the uncertainties of the calculation, the electron-nucleon and muon-nucleon axial vector coupling constants are the same.

## INTRODUCTION

SEVERAL authors<sup>1-3</sup> have recently discussed the weak interactions among spin  $\frac{1}{2}$  particles. A comparison of  $\beta$  decay and  $\mu$  decay reveals a close similarity between the electron-nucleon and muon-nucleon interactions: both are of the vector ( $V$ ) and axial vector ( $A$ ) form, and the  $V$  coupling constants for the two processes and the  $A$  constant for  $\mu$  decay appear nearly identical.<sup>1,2</sup> The  $A$  coupling constant for  $\beta$  decay has been shown experimentally to be 1.14 times larger than the  $V$  coupling constant; this difference is presumably due to a renormalization because of the virtual meson cloud of the nucleon.<sup>2</sup>

Whether the universality extends to the muon-nucleon interaction, i.e., whether the  $\mu$ -absorption process  $\mu^- + p \rightarrow n + \nu$  and the  $\beta$ -decay process  $n \rightarrow p + e^- + \bar{\nu}$  are governed by the same basic interaction, is not so well known. It is attractive to assume that the interactions of  $\beta$  decay and  $\mu$  absorption are the same, and that the  $V$  coupling constants of the two interactions are identical. The  $A$  coupling constant of  $\mu$  absorption is presumably then to be renormalized as was the  $A$  coupling constant of  $\beta$  decay, although the renormalization factor may be nearly unity.

The  $\mu$ -absorption and  $\beta$ -decay processes may be compared directly in the reactions



where the chemical symbols represent the ground states of the nuclei. The spin change is 1, so the selection rules are Gamow-Teller. The initial state of the muon-carbon system (1) is the ground state of the mesonic atom, so the process is analogous to  $K$  capture. In the

allowed approximation, the nuclear matrix elements are the same for (1) and (2), so that the ratio of the two rates may be calculated in terms of the ratio of the  $A$  coupling constants without assuming a nuclear model. In the present experiment, the rate of reaction (1) is measured and compared with the known rate of reaction (2). The theoretical calculations are complicated by the fact that forbidden transitions are important<sup>4</sup> in (1).

The reaction (1) was studied by Godfrey,<sup>5</sup> using a small liquid scintillation counter surrounded by Geiger tubes as a detector. He concluded that the muon-nucleon and electron-nucleon coupling constants were probably the same, within the experimental error. Now that the techniques of larger liquid scintillators are known, it seemed worthwhile to repeat the experiment.

## EXPERIMENT

The present experiment was a study of the absorption of cosmic-ray muons stopped in carbon. Liquid scintillation counters provided the "target" carbon nuclei with which the muons could interact, and the detectors with which the interactions were studied. The composition of the scintillator fluid was  $CH_{1.5}$ .

Negative mesons stopping in the detector slow down, are captured, and cascade down to the lowest bound state of a mesonic atom in a time of the order of  $10^{-10}$  sec. (Following Marshak, the word "capture" is used to denote the entering of a meson into an atomic bound state, while "absorption" denotes the penetration of a meson into the nucleus). All negative muons stopping in a hydrocarbon are captured into the lowest bound state of the carbon mesonic atoms in a time negligible compared to the muon mean life, so that the presence of hydrogen has no effect on the absorption process. Positive mesons are not captured by nuclei, and all positive mesons decay. About 90% of the stopped

<sup>†</sup> Work performed under the auspices of the U. S. Atomic Energy Commission.

<sup>1</sup> R. P. Feynman and M. Gell-Mann, *Phys. Rev.* **109**, 193 (1958).

<sup>2</sup> M. Gell-Mann, *Phys. Rev.* **111**, 362 (1958).

<sup>3</sup> M. L. Goldberger and S. B. Treiman, *Phys. Rev.* **111**, 354 (1958).

<sup>4</sup> K. W. Ford, private communication (to be published).

<sup>5</sup> T. N. K. Godfrey, *Phys. Rev.* **92**, 512 (1953); **94**, 756 (1954); thesis, Princeton University, 1954 (unpublished).

negative muons decay, the remaining 10% being absorbed by carbon.

The most important reactions of muons stopped in carbon are:

$$\mu^\pm \rightarrow e^\pm + \nu + \bar{\nu}, \tag{3}$$

$$\mu^- + C^{12} \rightarrow B^{12} + \nu, \tag{4}$$

$$\rightarrow B^{12*} + \nu, \quad B^{12*} \rightarrow B^{12} + \gamma, \tag{5}$$

$$\left. \begin{aligned} &\rightarrow B^{11} + n + \nu \\ &\rightarrow B^{10} + 2n + \nu, \text{ etc.} \end{aligned} \right\} \tag{6}$$

where  $B^{12}$  indicates the ground state, and  $B^{12*}$  an excited state. Figure 1 illustrates the reactions (4) through (6). The apparatus was designed to allow discrimination among the reactions (3), (4), (5), and (6).

A cylindrical tank, 115 cm in diameter by 115 cm high, was constructed of half-inch-thick polyethylene. Polyethylene was used instead of aluminum or steel because such metals, in capturing stray neutrons, would have given rise to high-energy gamma rays which would have constituted a serious background. The tank was divided into four compartments labeled 1, 2, 3b, and 3c as shown in Fig. 2. Compartment 2 (referred to below as tank 2) was a cylindrical volume 30 cm in diameter by 30 cm high. The walls of tank 2 and the two horizontal diaphragms were of cheese cloth impregnated with epoxy resin. All interior surfaces were painted with white Plasite paint (Wisconsin Protective Coating Company, Green Bay, Wisconsin). The vertical walls of tank 2 were 0.8 mm thick; the circular bottom was a sheet of Mylar, negligibly thick, and the bottom effectively consisted

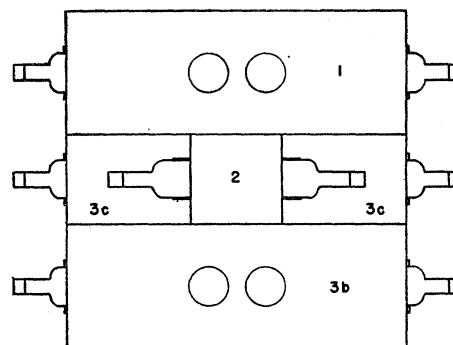


FIG. 2. Cross section of the detector. The outer wall formed a cylinder 115 cm in diameter and 115 cm high. Tank 2 was a cylinder 30 cm by 30 cm, centered in the larger volume. Tanks 1 and 3b were cylindrical; 3c was annular.

of 0.3 mm of paint. Tank 2 was viewed by two C-7170 photomultipliers. Tanks 1, 3b, and 3c each had eight 6364 photomultipliers, arranged in pairs so as to minimize the size of shield required. The large tank was filled to within a few centimeters of the top with a scintillator fluid consisting of triethyl benzene containing 3 g/l of terphenyl, with 0.1 g/l of POPOP as a wavelength shifter. All the photomultipliers in each section were connected in parallel, and when tanks 3c and 3b were operated as one detector, all 16 tubes were in parallel. The individual tube gains were balanced by adjusting the fraction of the overall supply voltage which appeared between the last dynode and the collector.

The detector was set inside a 1-ft-thick neutron shield, consisting of paraffin above and below, and water on the four sides. The water contained  $NaBF_4$  in solution, and the paraffin was mixed with borax. Outside the neutron shield was a layer of lead, 4 inches thick on the bottom and sides and 6 inches thick on top as a protection against gamma rays and electron showers. The assembly was located above ground, below a thin roof, at an elevation of 2200 m (atmospheric pressure of 800 g/cm<sup>2</sup>).

Most of the counts from the cosmic radiation were due to single particles at minimum ionization passing downwards through the detector. The pulse-height distribution in each tank showed a peak corresponding to the energy loss of a minimum-ionizing particle traversing the counter vertically. A sharper peak could be obtained by the use of coincidence techniques. The solid curve of Fig. 3 is the measured pulse-height distribution of pulses from tank 2 satisfying the requirement 1 2  $\bar{3}c$  (i.e., coincident pulses in 1 and 2 unaccompanied by a pulse in 3c, with tank 3b disconnected). Considering particles having a  $\cos^2$  angular distribution about the zenith, the most probable path length in tank 2 for those causing a 1 2  $\bar{3}c$  coincidence is the minimum one, i.e., the 30-cm height of the tank. Longer path lengths are distributed according to an  $x^{-4}$  law (neglecting edge effects) as indicated by the

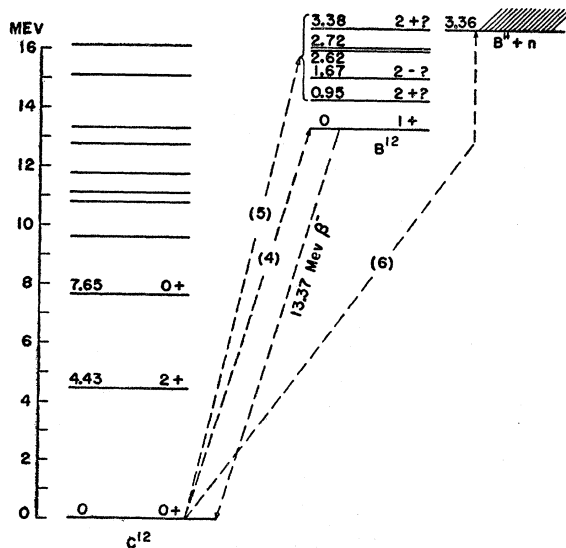


FIG. 1. Energy level diagram for  $C^{12}$  and  $B^{12}$ , illustrating the reactions (4), (5), and (6). It is thought that one of the two levels of  $B^{12}$  around 2.7 Mev is 0+, the transition from the ground state of  $C^{12}$  being unfavored. The  $\beta$  decay of  $B^{12}$  is 97% to the ground state of  $C^{12}$ , 3% to excited states.

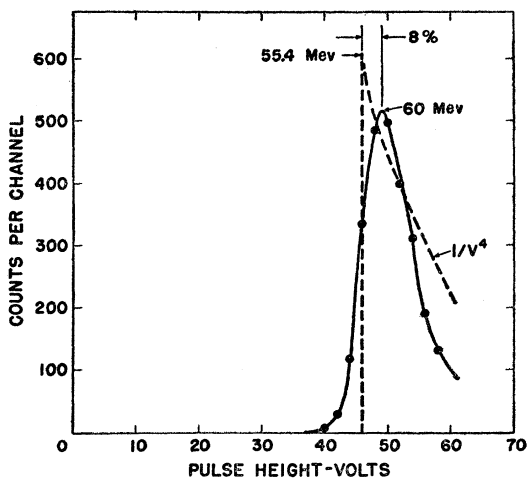


FIG. 3. Solid curve: experimentally observed pulse-height distribution of cosmic-ray pulses in tank 2 which satisfy the coincidence requirement  $12\bar{3}c$  (with  $3b$  disconnected). Dashed curve: predicted energy loss distribution for cosmic rays satisfying  $12\bar{3}c$  having a  $\cos^2$  distribution about the zenith. The solid curve is consistent with the dashed curve folded through a Gaussian resolution function of 8.5% full width at half maximum. The energy loss of a minimum ionization particle traversing the 30-cm minimum path in tank 2 is 55.4 Mev.

dashed curve of Fig. 3. The shift of the peak and the difference in shape between the two curves is due to the finite energy resolution of the system. The shape of the measured curve corresponds to a resolution of 8.5% full-width at half-maximum, resulting in an 8% shift in the position of the peak. The energy loss at minimum ionization for a path length of 30 cm is 55.4 Mev. The peak of the observed curve is 8% higher, or 60 Mev. This was the basis of the energy calibration in tank 2, and the other three tanks were calibrated similarly.

The C-7170 photomultipliers were found to be nonlinear for pulses as large as those made by mesons passing through tank 2. By putting screens with a light transmission of 11% in front of the tube faces, it was found that the pulse height corresponding to the through meson peak was reduced to 17% of its value without the screens. The ratio of 1.5 was used as a correction factor in setting the energy bounds in the coincidence circuit. The final energy calibration for small pulses in tank 2 was made on the basis of the end point of the  $B^{12}$ -decay-electron spectrum. It is discussed in the next section.

In the taking of data,  $3c$  and  $3b$  were connected in parallel and are referred to as tank 3. The muons studied were those which stopped in the scintillator in tank 2, producing a coincidence  $12\bar{3}$ . In the coincidence circuit, upper and lower bounds were imposed on the amplitudes of acceptable pulses. In tank 1, the limits were 60 and 120 Mev: this interval includes the energy losses of most muons which subsequently stop in tank 2, but excludes most of the stopping protons. (Tank 1 minimum ionization peak was at 70 Mev.) The accept-

able interval for tank 2 was from 25 to 150 Mev. The lower bound insured that a stopped muon must have penetrated a minimum of about 2.5 cm into tank 2 before it could be counted. Tank 3, which was in anticoincidence, had a lower bound of 4 Mev but no upper bound. (4-Mev muons have a range of 1.5 mm in the scintillator fluid.)

Pulses in the various sections of the detector were displayed on an oscilloscope triggered by the  $12\bar{3}$  coincidence circuit and photographed. To allow distinction among the different reactions (3) through (6), the beam was made to sweep across the scope face three times (Fig. 4). Sweep durations were 15  $\mu$ sec for trace 1, 400  $\mu$ sec for trace 2, and 0.1 sec for trace 3.

The most likely reaction for a stopped muon is its decay (3), with a mean life of 2.1  $\mu$ sec. The decay electron usually gave a pulse in tank 2, but for those mesons which stopped in or near the wall, the decay electron might leave little or no energy in tank 2, but give a pulse in tank 3. The 25-Mev lower bound in tank 2 for incoming particles insured that decay electrons travelling upwards would deposit a minimum of 4 Mev in tank 2. Pulses in tank 2 and 3 were displayed separately on trace 1 (Fig. 4). Nearly all (99.9%) of the muon decays occurred within the 15  $\mu$ sec of trace 1 and essentially all of the decay electrons gave detectable pulses in tank 2 or 3.

Next to decay, the most likely interaction of a stopped  $\mu^-$  is (6), in which one or more neutrons are liberated in tank 2 at a mean time of 2.0  $\mu$ sec after the entry of the muon. For these events there will be no decay electron pulse on trace 1, but there may be a small pulse from tank 2 or 3 due to recoil protons, or to any gamma rays which may be emitted by the residual nucleus. The neutron will probably be thermalized in

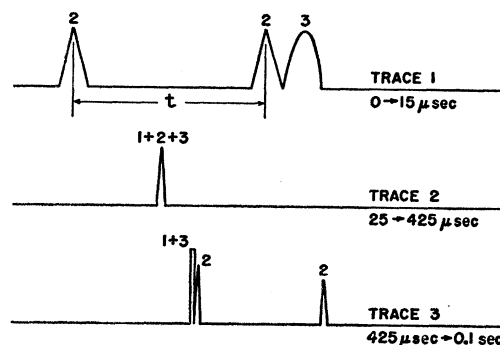


FIG. 4. Schematic representation of oscilloscope display. Numbers above the pulses indicate the tanks (Fig. 2) in which the pulses were generated. The first pulse on trace 1 is the trigger pulse  $12\bar{3}$ , and provides the time fiducial. On trace 1, the tank 3 pulses are delayed about 1  $\mu$ sec and displayed with a pulse shape different from tank 2 pulses to allow identification. A stopped muon decaying a time  $t$  after stopping in tank 2 would produce pulses in tanks 2 and 3 as indicated if the decay electron penetrated the wall of tank 2 into tank 3. On trace 3, tank 2 pulses are delayed and displayed with a pulse shape different from the pulses derived from tanks 1+3.

the large tank and captured in the hydrogen of the scintillator fluid, the resulting 2.2-Mev gamma ray being detected in one of the compartments of the detector. The mean neutron capture time is calculated to be 240  $\mu\text{sec}$ . The pulses from all compartments of the detector were added electronically and displayed on trace 2, which covered a time interval during which 73% of the neutron captures occurred.

When  $B^{12}$  is formed by muon absorption, by reaction (4) or (5), the  $B^{12}$  nucleus beta decays back to  $C^{12}$ , with a mean life of  $29.2 \pm 0.6 \text{ msec}$ <sup>6</sup> and an end-point energy of 13.4 Mev. The mean time for the formation of the  $B^{12}$  is 2.0  $\mu\text{sec}$ , which is negligible compared to the  $\beta$ -decay mean life. The pulses from tank 2 were displayed on trace 3, which covered a time interval during which 95% of the  $B^{12}$   $\beta$  decays occurred. If a pulse occurred in tank 1 and/or 3 in coincidence with a pulse from tank 2 which was shown on trace 3, the pulses from tanks 1 and 3 were added electronically and displayed just before the tank 2 pulse (Fig. 4). With this system pulses from charged cosmic-ray particles passing through tank 2 could be rejected in the film analysis, at the expense of losing those  $B^{12}$   $\beta$  rays which penetrated through the walls of tank 2.

If muon absorption to bound excited states of  $B^{12}$  occurred (5), the  $B^{12*}$  nucleus would immediately emit one or more gamma rays with a total energy between 0.95 and 3.38 Mev (Fig. 1). The time delay between the arrival of the muon and the gamma-ray emission would correspond to the mean life of the  $\mu^-$  in carbon, 2.0  $\mu\text{sec}$ . If the gamma ray were detected in Tank 2 or 3, a pulse would appear on trace 1. Pictures with a small second pulse on trace 1 and a pulse on trace 3 characteristic of  $B^{12}$  decay were identified as possibly due to process (5), and the number of  $B^{12*}$  events detected was used to correct the rate of transitions to the  $B^{12}$  ground state, using an estimate of the efficiency for the detection of the  $B^{12*}$  gamma rays.

Thirty thousand photographs of scope patterns were taken over a period of several weeks. The runs were made under two conditions, and were called  $\alpha$  and  $\beta$  runs. The  $\alpha$  runs were intended primarily to measure the rate of muons stopping in tank 2, and  $\beta$  runs to observe the interactions of stopped negative muons with carbon. In the  $\alpha$  runs, the scope was triggered by  $12\bar{3}$  coincidences, and the number of stopped muons was determined by observation of the number of  $\mu$ -decay electrons recorded. In the  $\beta$  runs, in order to conserve film and make the reading easier, an electronic circuit prevented photographing most of the muon decay events. This circuit rejected events in which a second pulse greater than 4 Mev occurred in tank 2 within 10  $\mu\text{sec}$  of the  $12\bar{3}$  coincidence, and it also reduced the frame rate from 5.5 per minute of  $\alpha$  runs to 1.5 per minute. The remaining muon-decay events were rejected visually (i.e., delays greater than 10  $\mu\text{sec}$ ,

<sup>6</sup> A. W. Schardt, preliminary results (private communication).

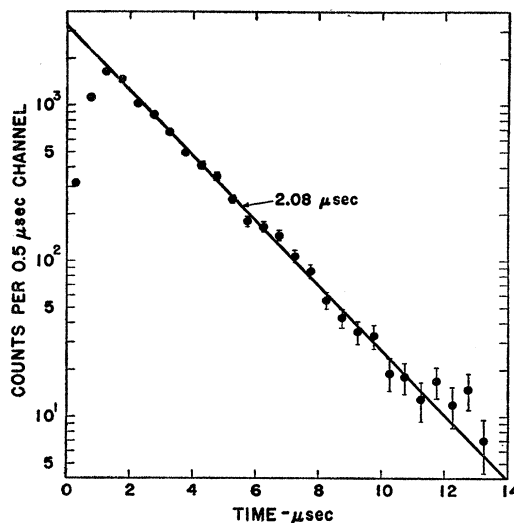


FIG. 5. Decay-time spectrum of stopped cosmic-ray muons. No background has been subtracted. The line corresponding to a mean life of 2.08  $\mu\text{sec}$  is the least-squares fit to the data beyond 1.5  $\mu\text{sec}$ . Standard deviations are shown except where they are smaller than the dots.

and events in which most of the decay electron energy was deposited in tank 3). The  $\alpha$  and  $\beta$  runs were alternated, with about the same total number of pictures in each.

## RESULTS

### $\mu^-$ Stopping Rate

The stopping rate of cosmic-ray muons in tank 2 was determined from the  $\alpha$  runs. The decay events were selected visually, and the time between the muon arrival and decay was measured ( $t$  of Fig. 4). The time scale was broken into 0.5- $\mu\text{sec}$  intervals and the number of events falling into each interval tallied. Figure 5 contains a plot of all the muon decays observed in the  $\alpha$  runs. No background has been subtracted. A least-squares fit of the function  $Ae^{-t/\tau}$  to the data beyond 1.5  $\mu\text{sec}$  gives a value  $\tau = 2.08 \pm 0.03 \mu\text{sec}$  for the mean life, where the error is statistical.<sup>7</sup> This mean life is characteristic of the cosmic-ray mixture of  $\mu^+$  and  $\mu^-$  stopped in carbon, and is in agreement with the accepted value<sup>8</sup> of  $2.12 \pm 0.02 \mu\text{sec}$ .

The total number of muons that stopped and decayed during the  $\alpha$  runs is the area under the curve in Fig. 5. Probably the area is obtained most accurately by using the accepted value of  $\tau = 2.12 \mu\text{sec}$  and performing a least-squares fit for  $A$ , the  $t=0$  intercept. Then the number of muons decaying in Tank 2 is  $N_0 = 2A\tau$

<sup>7</sup> All least-squares fits reported in this paper were made by the maximum likelihood method, and statistical errors were derived from the internal consistency of the data. We are indebted to R. H. Moore for performing these calculations.

<sup>8</sup> W. E. Bell and E. P. Hincks, Phys. Rev. 84, 1243 (1951); 88, 1424 (1952). Sens, Swanson, Telegdi, and Yovanovitch, Phys. Rev. 107, 1464 (1957); Lundy, Sens, Swanson, Telegdi, and Yovanovitch, Phys. Rev. Letters 1, 102 (1958).

(0.5- $\mu$ sec intervals have been used). The observed value is  $N_0 = 13\,200 \pm 530$ , where the indicated error contains both statistical and estimated systematic errors.

In the data, points for the first three 0.5- $\mu$ sec intervals in Fig. 5 have been neglected in the calculations. The efficiency for detecting decays in the first microsecond was low, partly because of difficulty of resolving pulses on the film, and partly because the decay electrons had a good chance of entering tank 3 and tripping the 3 circuit, making the event appear as a through muon instead of a stopped muon. The threshold for detection of the decay electrons was set at 0.2 Mev; the fraction of decay electrons having less than 0.2-Mev energy was negligible.  $N_0$  as calculated above needs no further correction for detection efficiency.

The rate at which negative muons stopped in tank 2 and were captured by  $C^{12}$  during the  $\alpha$  runs was

$$R_\mu = \frac{N_0(1-f)}{T_\alpha(1+r-\phi)} \text{ min}^{-1}, \quad (7)$$

where  $f$  = fraction of stopped  $\mu^-$  which are captured by nuclei other than  $C^{12}$ ,  $r$  = ratio of number of  $\mu^+$  to  $\mu^-$  in the incident cosmic-ray flux,  $\phi$  = fraction of stopped  $\mu^-$  which absorb in nuclei instead of decaying, and  $T_\alpha$  = total running time of the  $\alpha$  runs = 1727 min.

The fraction  $f$  is estimated to be  $0.03 \pm 0.01$ . The natural abundance of  $C^{13}$  contributes  $\frac{1}{3}$  of this value, and the remainder comes from the heavy material in the vicinity of tank 2. The ratio  $r$  is measured as  $r = 1.22 \pm 0.02$  around the zenith at sea level and is calculated to be 1.3 near the top of the atmosphere.<sup>9</sup> The value  $r = 1.23 \pm 0.05$  is used in Eq. (7) as appropriate to 2200 m elevation. The fraction  $\phi$  is calculated from the mean life of  $\mu^+$  and  $\mu^-$  in carbon and is  $0.09 \pm 0.02$ . Substitution of the above numerical values in Eq. (7) gives  $R_\mu = 3.46 \pm 0.18$  stopped negative muons per minute. The indicated error contains both statistical and estimated systematic errors.

The above  $\mu^-$  stopping rate is taken as the average over the course of the experiment since the  $\alpha$  and  $\beta$  runs were alternated. The  $\beta$  runs were monitored by registers which recorded the number of muon decay events not photographed. There were no significant deviations in the rates of the  $\alpha$  or  $\beta$  runs.

#### $\mu^-$ Absorption Rate

The rate of events in which negative muons were absorbed to the ground state of  $B^{12}$  was deduced from the  $\beta$  runs. A picture was accepted if it passed the following tests: (i) no second pulse on trace 1 greater than 0.5 Mev; (ii) a pulse on trace 3 with between 4 and 15 Mev in tank 2, not accompanied by a pulse in tank 1 or 3. These pictures were due to the following types of events:

- (a)  $\mu^-$  absorption to  $B^{12}$  (4);
- (b)  $\mu^-$  absorption to one of the bound excited states of  $B^{12*}$  (5), and failure to detect the gamma ray emitted in the transition to  $B^{12}$ ;
- (c) a random coincidence between a first pulse satisfying the selection criteria and an unrelated pulse on trace 3 satisfying the criteria for a  $B^{12}$  electron.

The pulses on trace 3 in events of type (a) and (b) had the time and pulse-height spectra characteristic of  $B^{12}$  decay. Those of type (c) had a uniform time distribution. The distribution of delay times from the pictures accepted on the basis of the above tests is shown in Fig. 6.

The background level for the data shown in Fig. 6 was estimated as follows: the function  $a + be^{-t/\tau}$  was fitted to the data by least squares, the value of  $\tau$  being fixed at the known mean life of  $B^{12}$ , and  $a$  and  $b$  being free parameters. Those frames in the  $\beta$  runs with second pulses on trace 1 were analyzed in the same way: these were presumed to include muon decays and possibly  $B^{12*}$  events (5). The value of  $a$  in these two calculations gave a measure of the background. In addition, the random rate was calculated for the muon decays in the  $\alpha$  runs, which had a time distribution of pulses on trace 3 which was flat within statistics. The weighted mean of these three values of  $a$  was taken to be the best estimate of the random background. Another fit was now made to the data, Fig. 6, this time keeping  $a$  and  $\tau$  fixed and allowing only  $b$  to vary. This gave  $73.4 \pm 4.2$  as the best estimate of the expected number of counts in the first 4 msec. The total number of  $B^{12}$  decays recorded, corrected for losses at early and late times, was 574.

If  $\mu^-$  absorption does occur an appreciable fraction of the time to excited states of  $B^{12*}$ , which are stable with respect to neutron emission, thus will contribute to the measured  $B^{12}$  decay rate. The transitions to the

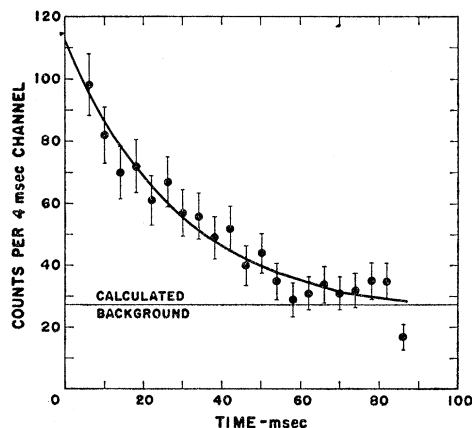


FIG. 6. Time-delay spectrum of pulses on trace 3 satisfying selection criteria for  $B^{12}$  decay electrons. Errors shown are standard deviations. The curve is the least-squares fit of the function  $a + be^{-t/\tau}$  with  $\tau$  fixed at the known  $B^{12}$  mean life, and  $a$  fixed at the calculated value.

<sup>9</sup> Fasoli, Modena, Pohl, and Pohl-Ruling, Nuovo cimento 6, 869 (1957).

bound excited states (5) were treated in the same way as those to the ground state (4), except that the requirement was made that there be a second pulse on trace 1, either in tank 2 or 3, in the energy range 0.5 to 4 Mev. The time distribution of the pulses on trace 3 is shown in Fig. 7, for events having a small second pulse on trace 1. There is an indication of a component with a mean life of the order of 30 msec. If we take this to be due to  $B^{12*}$ , we find the total number of  $B^{12*} \rightarrow B^{12} \rightarrow C^{12}$  decays recorded was  $33 \pm 11$ .

The efficiency for the detection of a 2-Mev gamma ray was calculated to be 0.80.  $B^{12*}$  counts were recorded as  $B^{12}$  because of the escape of the gamma ray, and also when the gamma-ray pulse on trace 1 came so close to the first pulse that it could not be resolved. The loss of counting efficiency from the latter cause was determined by plotting the time distribution of all second pulses on trace 1 in the energy range 0.5 to 4 Mev. The data were fitted to a constant pulse an exponential with a decay time of  $2.0 \mu\text{sec}$ . From the number of counts missing in the first microsecond the fraction lost at early time was found to be 0.23. The over-all detection efficiency for  $B^{12*}$  gamma rays was taken to be  $0.80 \times 0.77 = 0.62$ . The total number of  $B^{12*}$  events was therefore  $53 \pm 17$ , of which 21 were counted as  $B^{12}$  events. This leaves  $N_B = 553$  as the net number of  $B^{12}$  events.

The statistics are such that it cannot be claimed definitely that transitions (5) to the bound excited states of  $B^{12*}$  were recorded. From the data, it seems likely that such transitions did occur about 10% as often as to the ground state, and so we have made the correction, which fortunately was small.

The number of  $\mu^-$  absorption events per minute to the ground state of  $B^{12}$  was

$$R_B = \frac{N_B}{T_B \epsilon_B (1-L)(1-R_\theta t_\theta)(1-G)} \text{ min}^{-1}, \quad (8)$$

where  $N_B$  = number of  $B^{12}$  events = 553;  $T_B$  = total running time of the  $\beta$  runs = 13 091 min;  $L$  = probability

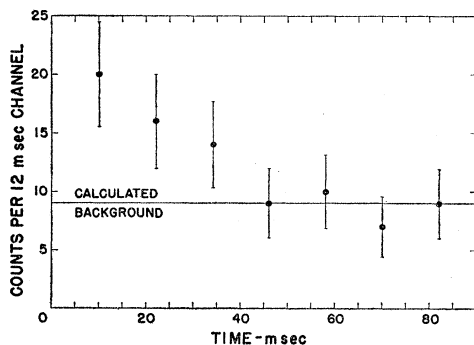


Fig. 7. Time-delay spectrum of pulses on trace 3 satisfying selection criteria for  $B^{12*}$  decay electrons. Errors shown are standard deviations. The data have been lumped into 12-msec channels because of the small number of counts.

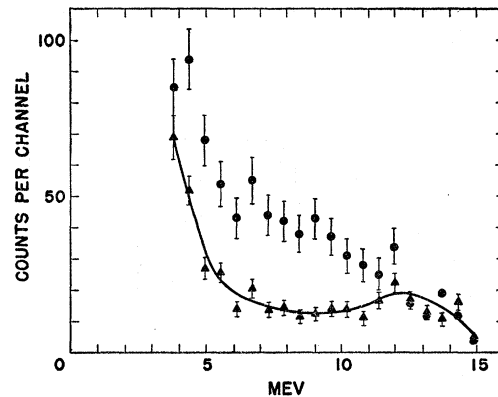


Fig. 8. Pulse-height distribution of pulses on trace 3. The circles represent pulses satisfying the criteria for  $B^{12}$ -decay electrons. The triangles represent background pulses taken from muon-decay events. Errors shown are standard deviations. The curve is a visual fit to the background data.

that the  $B^{12}$  decay electron will penetrate the wall of tank 2 and therefore be rejected, calculated to be 0.07;  $R_\theta$  = number of pulses per millisecond on trace 3 due to particles passing through the counter, measured to be 0.045;  $t_\theta$  = dead time per pulse on trace 3, estimated to be 0.3 msec;  $G$  = chance that a pulse from tank 2 will be accompanied by an unrelated pulse in 1 or 3, and therefore be accidentally rejected (the measured value of  $G$  is 0.01); and  $\epsilon_B$  = probability that the  $B^{12}$  decay electron should give a pulse between 4 and 15 Mev, obtained from an analysis of the pulse height spectrum of the  $B^{12}$  decay electrons.

Figure 8 is the pulse height spectrum of the pulses occurring in the first 44 msec of trace 3 in events satisfying the  $B^{12}$  decay criteria. The background was deduced from the pictures showing a muon decay. The net spectrum is shown in Fig. 9. The curve in Fig. 9 is the known shape of the  $B^{12}$   $\beta$ -decay spectrum,<sup>10</sup> corrected for edge effects and normalized along both axes. As mentioned above, the tank 2 photomultipliers were nonlinear at large pulse heights ( $\sim 60$  Mev), so that the pulse-height calibration from the through peak could not be used directly in the region of a few Mev. A correction for the nonlinearity was made in setting the thresholds, but it was found that the most accurate energy calibration for events of a few Mev in tank 2 was that obtained from the  $B^{12}$  decay electron spectrum. The energy scale shown in Fig. 9 agrees to within 15% with the corrected energy calibration from the through peak, which is considered satisfactory. The threshold for the acceptance of a pulse as a  $B^{12}$  decay electron was set at 4 Mev, which is the boundary between the first and second channels of Fig. 9. The efficiency  $\epsilon_B$  was calculated to be 0.74.

Substitution in Eq. (8) gives  $R_B = 0.0628$ . The error in  $R_B$  comes from the following sources:

<sup>10</sup> W. F. Hornyak and T. Lauritsen, Phys. Rev. **77**, 160 (1949).

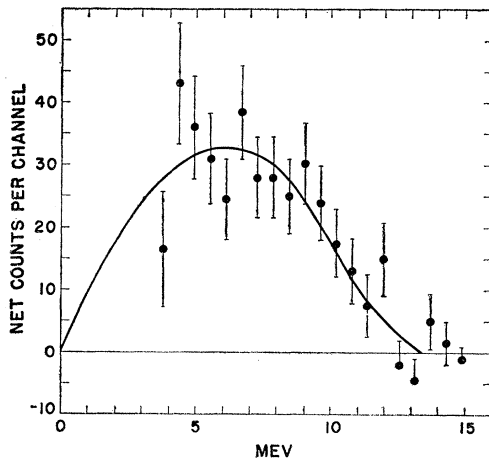


FIG. 9. Net pulse-height spectrum of pulses on trace 3 satisfying the criteria for  $B^{12}$  decay electrons. Errors shown are standard deviations. The curve is the known  $\beta$  spectrum of  $B^{12}$ , corrected for the fact that higher energy electrons are more likely to escape into tank 3 and therefore be rejected, and normalized along both axes. The points are those of Fig. 8 with the smooth curve subtracted.

(A) The number  $N_B$  was derived from the parameter  $b$  in the function  $a+be^{-t/\tau}$ , which was fitted to the data by least squares. The value of  $b$  derived from the fit was  $73.4 \pm 4.2$ .

(B) Similarly, the value of  $b^*$  to the  $B^{12*}$  data was  $b^* = 4.2 \pm 1.4$ . The correction to the value of  $b$  due to the inefficiency in recording  $B^{12*}$  gamma rays was  $2.6 \pm 0.8$ , so that  $b = 70.8 \pm 4.3$ . The error from (A) and (B) was 6.0%.

(C) In the fit of the function  $a+be^{-t/\tau}$ , it was assumed that  $a$  was known exactly. The calculated value of  $a$  was  $31.3 \pm 2.4$ . This uncertainty in the value of  $a$  causes an error in  $R_B$  of 7.4%.

(D) The uncertainty of 2% in the value of  $\tau$  results in an error in  $R_B$  of 1.1%.

(E) The efficiency  $\epsilon_B$  is uncertain because the energy scale, and hence the threshold energy for the acceptance of  $B^{12}$ -decay-electron pulses, are not known exactly. The curve in Fig. 9 was fitted to the points by least squares, and the uncertainty in the energy scale was found to be 3.1%. To take care of possible systematic errors, this was increased to 5%. This gave an error of 3.0% in  $\epsilon_B$ , and hence also in  $R_B$ .

The errors quoted above are statistically independent, and we may therefore take the over-all error to be square root of the sum of the squares of the individual errors. This is 9.6%, so that  $R_B = 0.063 \pm 0.006 \text{ min}^{-1}$ .

As a check, the mean life of  $B^{12}$  was calculated by fitting the function  $a+be^{-t/\tau}$  to the data shown in Fig. 6, keeping  $a$  fixed and taking  $b$  and  $\tau$  as free parameters. This gave  $\tau = 26.5 \pm 2.4 \text{ msec}$ , which is consistent with the known value.<sup>6</sup>

It is possible that  $\beta$ -emitting nuclei other than  $B^{12}$  might have been formed by interaction of the cosmic rays with carbon. Nuclei such as  $Li^8$  will not be confused

with  $B^{12}$  because of their long mean life. The only nuclide likely to be confused with  $B^{12}$  is  $N^{12}$ , which has a mean life of about 16 msec and an end-point energy of about 17 Mev.  $N^{12}$  can be formed by fast cosmic-ray protons in the reaction  $C^{12}(p,n)N^{12}$ . The rate of production of  $N^{12}$  was probably small compared to the rate of formation of  $B^{12}$  by muon absorption in  $C^{12}$ , and no correction for  $N^{12}$  has been made to the data.

### Neutrons

Whenever  $\mu^-$  absorption in  $C^{12}$  produced one or more neutrons (reaction 6), these neutrons were detected with an efficiency of  $85 \pm 5\%$ .<sup>11</sup> In order to gain information about the rate of reaction (6), the time delay and pulse height of pulses on trace 2 were recorded for events in the  $\beta$  runs having no decay-electron pulse on trace 1. The background on trace 2 was deduced from muon-decay events in the  $\alpha$  runs. The time-delay spectrum of the signal was consistent with the calculated mean capture time of 240  $\mu\text{sec}$  for neutrons in the scintillator, and the pulse-height spectrum was peaked at about 2 Mev, corresponding to the 2.2-Mev neutron-capture gamma-ray of hydrogen. The background time spectrum was flat, and the background pulse-height spectrum did not show the 2-Mev peak. The probability for a random neutron-like pulse on trace 2 was 22%.

It was possible for other cosmic-ray events to produce the same pattern of pulses as (6). For instance, a fast proton could undergo charge exchange in tank 2, the fast neutron passing undetected through tank 3. Associated with the fast proton entering the system might be several neutrons, which would be captured with the same characteristic time distribution as the neutrons from (6). For this reason a determination of the over-all absorption rate for negative muons in  $C^{12}$  was not possible, but an upper limit may be set. The observed neutron-production rate in events indistinguishable from (6) was  $0.55 \pm 0.05 \text{ min}^{-1}$ . Dividing this rate by the  $\mu^-$  stopping rate of  $3.46 \text{ min}^{-1}$  gives 0.16 for the number of neutrons generated per stopped  $\mu^-$ . The upper limit for the fraction of stopped negative muons which absorb in carbon to give free neutrons is therefore 16%.

The number of neutron pulses per frame was examined in an attempt to determine whether more than one neutron was emitted in some cases. The frequency distribution was found to be consistent with a neutron multiplicity of 1, although a multiplicity of 1.2 is not excluded.

The number and multiplicity of neutrons observed is thought to be consistent with the prediction from the known total absorption rate of  $\mu^-$  in carbon plus a reasonable contribution from other cosmic-ray-initiated events.

<sup>11</sup> G. I. Bell (private communication).

## DISCUSSION

The transition probability per unit time for the reaction  $\mu^- + C^{12} \rightarrow B^{12} + \nu$  (4) is given by

$$\Lambda_\mu = (R_B/R_\mu)(1/\tau_\mu), \quad (9)$$

where  $R_B$  = observed number of transitions via reaction (4) =  $0.063 \pm 0.006 \text{ min}^{-1}$ ,  $R_\mu$  = observed number of  $\mu^-$  mesons stopping<sup>12</sup> =  $3.46 \pm 0.18 \text{ min}^{-1}$ , and  $\tau_\mu$  = mean life of stopped  $\mu^-$  mesons in C =  $2.01 \pm 0.02 \text{ } \mu\text{sec}$ . Substitution gives  $\Lambda_\mu = 9050 \pm 950 \text{ sec}^{-1}$ .

Godfrey<sup>5</sup> found a total transition probability per unit time of  $(6.5 \pm 1.5) \times 10^3 \text{ sec}^{-1}$  for transitions to ground and bound excited states of  $B^{12}$ . If we take the contribution of the bound excited states to be 10% of the transition probability to the ground state, the comparable rate from the present experiment is  $(10 \pm 1) \times 10^3 \text{ sec}^{-1}$ , which is in rough agreement with Godfrey's result.

Since the reaction studied is the inverse of the beta decay of  $B^{12}$  to the ground state of  $C^{12}$ , except for the substitution of a muon for the electron, the nuclear matrix elements are equal in the first approximation. From a comparison of the rates of muon absorption and beta decay, it would be possible to determine the ratio of the muon-nucleon and electron-nucleon (axial vector) coupling constants, independently of the nuclear model.

<sup>12</sup> Not all the muons stopping in tank 2 were detected because of the restricted solid angle and the pulse-height limits imposed in the 123 circuit. This does not affect the ratio  $R_B/R_\mu$ .

The mean life for beta decay of  $B^{12}$  is  $29.2 \pm 0.6 \text{ msec}$ ,<sup>6</sup> with 97% of the transitions<sup>13</sup> going to the ground state of  $C^{12}$ . The transition rate to the ground state is therefore  $\Lambda_\beta = 33.2 \pm 0.65 \text{ sec}^{-1}$ . The ratio of transitions between the two ground states is

$$\Lambda_\mu/\Lambda_\beta = 273 \pm 29.$$

Because of the high energy available in muon absorption, the wavelength of the outgoing neutrino is not large compared to the nuclear radius, and forbidden transitions make an important contribution to the muon absorption rate. A preliminary calculation of the  $\mu^-$  absorption rate including contributions from forbidden transitions has been made by Ford.<sup>4</sup> The conclusion is that the above experimental results are compatible with a ratio of unity for the axial vector coupling constants, but that the limits which can be set on this ratio depend upon the nuclear model adopted.

Recent preliminary results of two groups<sup>14</sup> appear to confirm Godfrey's<sup>5</sup> measurement of the absorption rate of stopped negative muons in carbon to  $B^{12}$  via both the ground and bound excited states of boron, and are in rough agreement with the present result.

<sup>13</sup> Cook, Fowler, Lauritsen, and Lauritsen, *Phys. Rev.* **111**, 567 (1958).

<sup>14</sup> Fetkovich, Fields, and McIlwain; and Love, Marder, Nadelhaft, Seigle, and Taylor, Conference on Weak Interactions, Gatlinburg, Tennessee, October, 1958 [*Bull. Am. Phys. Soc. Ser. II* (to be published)].